ChemComm

Accepted Manuscript

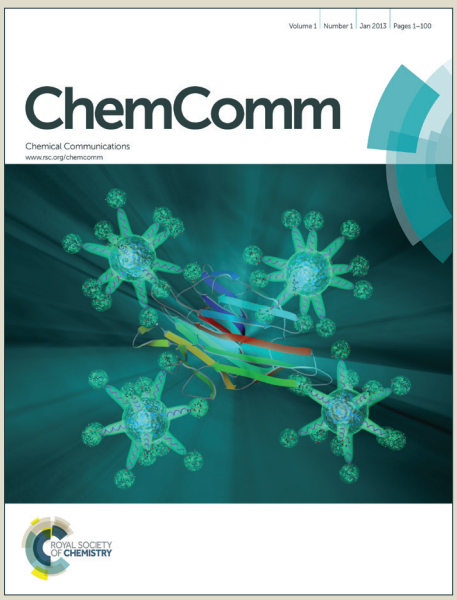

ROYAL SOCIETY OF CHEMISTRY

www.rsc.org/chemcomm

ChemComm

RSCPublishing

COMMUNICATION

Azeotropic Distillation Assisted Fabrication of Silver Nanocages and Their Catalytic Property of Reduction of 4-Nitrophenol

Cite this: DOI: 10.1039/x0xx00000x

Received 00th January 2012,
Accepted 00th January 2012

DOI: 10.1039/x0xx00000x

www.rsc.org/

Jianzhong Min,[a] Fei Wang,[a] Yunliang Cai,[a] Shuai Liang,[a] Zhenwei Zhang,[b] Xingmao Jiang*[a]

Monodisperse silver nanocages (AgNCs) with specific interiors were successfully synthesized by an azeotropic distillation (AD) assisted method and exhibited excellent catalytic activities for reduction of 4-nitrophenol (4-NP) into 4-aminophenol (4-AP) due to the unique hollow morphology and small thickness of the silver shell.

Noble metallic nanoparticles with hierarchical structure have garnered sustained research interest due to their superior metamaterial,[1] surface enhanced Raman scattering,[2] electronic,[3] catalytic,[4] biosensing and diagnosis properties.[5] Among these noble metalss, Ag is particularly attractive because of its lower cost and particularly, its superior catalytic properties of high reactivity and selectivity. In comparison to other noble metals Ag nanoparticles (AgNPs) demonstrated excellent catalytic performance for oxidative conversion of methanol into formaldehyde,[6] ethylene epoxidation,[7] hydrogenation of dimethyl oxalate[8] and so on. The aforementioned unique properties are strongly dependent on the size and nanostructures of AgNPs which can be fine-tuned to meet the demands of specific applications. A number of Ag particle morphologies such as wires,[9] cubes,[10] and spheres[11] have been successfully fabricated by varying techniques. Hollow Ag nanostructures have been attracting increasing attentions because they exhibit far different surface plasmonic properties and catalytic activities than their solid counterparts, and various hollow Ag nanostructures have been reported. Tang and co-workers[12] demonstrated a water-soluble sacrificial salt-crystal-template (SCT) method to assemble porous nanostructures with hollow interior morphologies, which included injecting saturated NaCl aqueous solution into anhydrous ethanol to prepare SCT NaCl templates, adding polyvinyl pyrrolidone (PVP) protected $AgNO_3$ solution, photo reduction or ethylene glycol-assisted reduction, and removal of the NaCl templates by water dissolution. Compared with conventional templating methods, the advantages of using NaCl as the template include low fabrication cost, abundance of NaCl and ease of removal of the template via dissolution, however, the drawback is the difficulty in controlling the size and size distribution of the NaCl crystals because drastically decrease of the NaCl solubility from water to ethanol lacks a good control of the NaCl grain growth resulting in fast formation of polydisperse NaCl crystals, and therefore, the Ag@AgCl cubes finally obtained were polydisperse and micrometer-sizes.

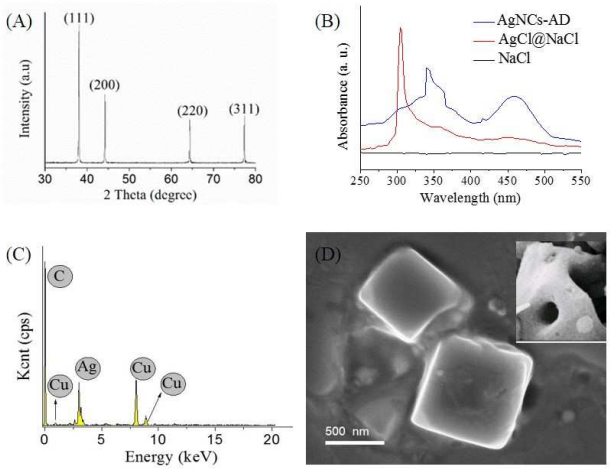

Fig. 1 (A) XRD pattern of AgNCs-AD. (B) UV-vis absorption spectra of AgNCs-AD, AgCl@NaCl and NaCl samples. C) EDS spectrum of AgNCs-AD shows that Ag is the only constituent elements of cages and copper, carbon elements come from the carbon-coated copper grid support film. (D) Typical SEM image of AgNCs-AD, the inserted image is a broken piece of the sample, showing the hollow interiors of the cubic cages.

Here we reported a facile and versatile approach to fabricate Ag nanocages (AgNCs) with well-defined hollow interiors and well-controlled size using NaCl nanocrystals as the templates.

The size-turnable NaCl cubes (50-500 nm) can be formed by an azeotropic distillation of a reverse microemulsion (aqueous NaCl droplets dispersed in benzene), and each NaCl crystal can be formed from one single aqueous droplet in the microemulsion after evaporation and removal of water. Based on these monodisperse NaCl templates, Ag nanocages can be facilely obtained through the reaction of $AgNO_3$ and the NaCl, reduction of AgCl, and removal of the NaCl templates. The size of the NaCl crystals can be controlled by initial aqueous droplet size and NaCl concentration in the reverse microemulsion, and as a result of uniform size of droplets in the microemulsion, the resulting NaCl crystals are monodispersed in size.

The XRD patterns of as-prepared AgNCs-AD were shown in Fig. 1A. The diffraction peaks with 2 θ values of 38.7, 44.7, 65.1, 77.9^o correspond to the (111), (200), (220), and (311) planes, which can be indexed to the face-centered cubic (*fcc*) structure of silver (JCPDS 36-1451). It is worth noting that there is no NaCl and AgCl diffraction peaks, indicating that all NaCl crystals were washed away and removed completely. To further examine the chemical status of the products, XPS spectra was shown in Fig. S1, see ESI†. Two peaks were observed at 368.2 and 374.2 eV, which can be ascribed to $Ag3d_{5/2}$ and $Ag3d_{3/2}$ peaks, respectively.[13] Moreover, the splitting of the 3d doublet of Ag was 6.0 eV, which indicates that these AgNCs-AD only contain metallic Ag (Ag^0).

Fig. 1C presented the Energy Dispersive Spectrometer (EDS) of the obtained AgNCs-AD, which indicated the presence of silver without NaCl or AgCl, was consistent with XRD results. The morphology of as-prepared AgNCs-AD was further studied by TEM and SEM. Fig. 1D shows that cubic-shaped Ag particles with a size of about 500 nm were found. However, attempts to observe the hollow structures though TEM were not successful as the walls of as-prepared Ag nanocages are too thick to be penetrated by the electron beam or too thin and unstable under intense electron beam irradiation (Fig. S2, see ESI†). As shown in Fig. 1D from the inserted image, a broken piece of the sample clearly demonstrated the hollow interiors of the cubic cages. These result suggested that as-prepared AgNCs-AD was hollow structure. Additionally, we investigated effect of the different ratio of water and Aerosol OT (AOT) added on the morphology and size of as-synthesized AgNCs-AD (Fig. S3, see ESI†). When the ratio of water and AOT increased from 5 : 1 to 20: 1, the size of as-synthesized NaCl crystal increased from ~20 nm to ~200 nm and accordingly the size of Ag@NaCl also increased. These results indicated that the control over the sizes of the nanocages was achieved by adjusting the ratio of water and AOT in the precursor. UV-vis absorption spectra of various samples was shown in Fig. 1B. The absorption of UV light (~308 nm) for AgCl@NaCl was due to large band gap energy of AgCl, while NaCl crystals show no absorption peak in the region. The limited absorption for AgCl@NaCl in the visible region might be due to the small amount of elemental Ag formed by room light illumination during preparation.[10] In general, silver nanospheres exhibited one UV absorption peak at around 430 nm, however, Ag nanocages displayed three surface plasmon resonance (SPR) absorption peaks located at 340, 415, 460 nm, respectively. This is because the number of SPR peaks increased as the symmetry of particles decreased: spherical particles have only one peak, whereas three peaks are often observed for cubic ones.[14] The strong absorption in visible region was due to the localized surface plasmon resonance and interband UV excitation of Ag nanoparticles, which explained well the enhancement of the catalytic performance.[15] This result proved that as-synthesized AgNCs-AD was cubic-structure, which agreed with SEM and TEM results.

To study the formation mechanism of Ag nanocages, XRD results of the intermediates at different synthesis stages were shown in Fig. S4, see ESI†. After azeotropic distillation process, the crystalline phase was assigned to cubic phase of NaCl (JCPDS 05-0628). Then adding $AgNO_3$ with complexation of N-octylamine, XRD pattern of the product showed AgCl@NaCl. Finally, the diffraction lines of the product by reducing were assigned to Ag@NaCl. The much low NaCl peaks intensities in Ag@NaCl were due to part of NaCl dissolved in water generated during the restore process.

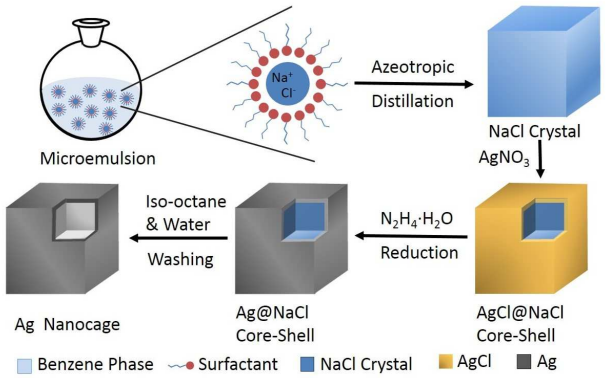

Scheme 1 Schematic illustration of the azeotropic distillation assisted (AD) route for the formation of Ag nanocage.

On the basis of the above experimental results and analysis, a possible mechanism for fabrication of Ag nanocages is elucidated schematically in Scheme 1. Firstly, ultrasonic treatment and magnetic stirring of the heterogeneous solution in the presence of surfactant generate a reverse microemulsion (water in oil). It is known that for the interfacial phenomenon reason, a plurality of NaCl aqueous solution droplets tend to disperse mono-sized and uniformly in a benzene phase.[16] In the distillation process of reverse microemulsion, water can be gradually removed from the droplets in the form of water/benzene azeotrope and cubic NaCl crystals can be formed within the interfacial film after a process of NaCl concentrating, saturation, and crystallization. The relatively slow evaporation process makes Na^+ and Cl^- ions have enough time for diffusion, crystallization or dissolution. The relatively large stable nucleus size for NaCl and small droplet size determines that, once a stable nucleus forms, the remaining droplet becomes substantially depleted in Na^+ and Cl^-, which reducing the possibility of multinuclear formation incident.[17,18] Furthermore, even if multiple nuclei were to form, Ostwald ripening would start to dissolve smaller NaCl crystallites and favors growth of larger one, eventually forming only one large, stable NaCl crystal in each droplet. Surfactant micelles along with complexation of N-octylamine with added $AgNO_3$ play an important role in preventing fast ion exchange, diffusion and reaction between NaCl and $AgNO_3$ and continued growth of AgCl on the surface of the NaCl crystal templates. As a result, the shell thickness is relatively constant and the outer and inner shell surface is smooth for each cubic AgCl@NaCl core-shell structure. Moderate reducing conditions and

support of the NaCl hard template may also be conducive to get the smooth surface for final hollow cubic structures.

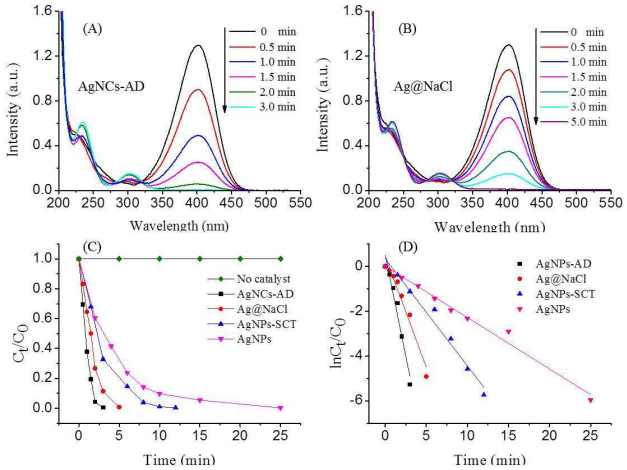

Fig. 2 Time-dependent UV-vis absorption spectra of the reduction of 4-NP by $NaBH_4$ in the presence of (A) AgNCs-AD and (B) Ag@NaCl as catalysts. (C) Plot of C_t/C_0 and (D) $\ln(C_t/C_0)$ versus reaction time for the reduction of 4-NP with different catalysts. C_0 and C_t was the absorption peak at 400 nm initially and at time (t). Conditions: [4-NP] = 5 mM; [catalysts] = 0.944 mg ml^{-1}; [$NaBH_4$] = 100 mM, 25 ℃.

The catalytic performance of as-prepared hollow AgNCs-AD was investigated by reduction reaction of 4-NP into 4-AP with an excess amount of $NaBH_4$. For comparison, Ag@NaCl nanoparticles (NaCl was not wash away), AgNPs-SCT and AgNPs (about 5 nm, Fig. S5, see ESI†) were also investigated (Fig. 2). Fig. 2 shows the time dependent catalytic process monitored by UV-vis spectroscopy using different catalysts. Generally, pure 4-NP shows a distinct spectral profile with an absorption maximum at 316 nm and the mixture of 4-NP and $NaBH_4$ shows a strong adsorption peak at 400 nm due to the formation of 4-nitrophenolate ion.[19] As shown in Fig. 2A, with the reaction time prolonged, the peak intensity of 4-NP gradually decreased and the peak intensity of 4-AP increased for AgNCs-AD sample accordingly. After 3 min, the absorption peak at 400 nm for 4-NP disappeared, while the absorption peak of 4-AP reached the maximum value, indicating that a complete conversion of 4-NP to 4-AP. In comparison to other samples, the reduction time for complete conversion of 4-NP to 4-AP for AgNCs-AD was much shorter than Ag@NaCl (5 min), AgNPs-SCT (12 min), AgNPs (25 min) counterparts (Fig. 2C). Furthermore, the isosbestic points were fixed at around 315 nm, indicating that the reduction proceeded without formation of byproducts.[20] In case of excess $NaBH_4$ was used, the pseudo-first-order rate law could be applied in order to quantitatively compare the catalytic activity of above catalysts.[21] The plots of $\ln(C_t/C_0)$ vs. the reaction time (t) for the catalysts are shown in Fig. 2D, and the corresponding value of k was calculated from the slope as summarized in Table 1. It is obvious that the catalytic activities of the catalysts decrease in the order AgNCs-AD > Ag@NaCl > AgNPs-SCT > AgNPs. According to previous reports, sharper, rougher edges and corners in both the inner and outer surfaces have more valency-unsatisfied surface atoms to act as active sites,[22] and compared to the catalyst prepared with SCT method, smaller size and narrower size distribution of our catalyst (~200 nm) greatly enhanced size-dependent catalytic property, which explained well why NaCl removal improves almost doubled catalytic performance and AgNCs-AD shows better activity than AgNPs-SCT. AgNPs showed the worst catalytic performance because nano-sized Ag particles were easily aggregate to decrease their higher surface energy, resulting in a remarkable reduction in their catalytic activities and dispersion stability.

Table 1 Summary of the reaction rate constants (k) of the catalysts

Catalysts	AgNPs-AD	Ag@NaCl	AgNPs-SCT	Ag NPs
k (min^{-1})	1.8	1.0	0.48	0.23

In summary, we developed an azeotropic distillation assisted process for preparation of monodisperse size-controlled Ag nanocages that show superior catalytic performance for the reduction of 4-NP to 4-AP by $NaBH_4$ than Ag@NaCl, AgNPs-SCT, and AgNPs. More importantly, our work not only demonstrated their potential applications in catalytic reduction of 4-NP, but also provided a new general method to fabricate other hierarchical monodisperse particles with cubic hollow nanostructures. It is expected that by selecting other salts such as nitrates of Zn, Cd, Cu, Au, Ag etc. instead of NaCl and using thiourea, NaOH and water soluble surfides orhalides instead of $AgNO_3$ as the reactant on the interface, a number of core-shell or hollow cubic functional nanomaterials such as sulfides (ZnS, CdS), halides, oxides, metals/alloys can be fabricated for a wide range of applications.

Acknowledgments

This work was financially supported by the National Natural Science Foundation of China (Nos. 21373034, 21201140), the Specially Hired Professorship-funding of Jiangsu Province (No. SCZ1211400001), Key University Science Research Project of Jiangsu Province (No. 13KJA530001) and the Start-up Funds from Changzhou University of Jiangsu Province, Jiangsu key Laboratory of Advanced Catalytic Material and Technology and PAPD of Jiangsu Higher Education Institutions.

Notes and references

[a] *Key Laboratory of Advanced Catalytic Material and Technology, Changzhou University, Changzhou 213164, PR China. Fax: +86-519-8633-0251; Tel: +86-519-8633-0253*
E-mail address: jxm@cczu.edu.cn
[b] *State Key Laboratory of Materials-Oriented Chemical Engineering, College of Chemistry and Chemical Engineering, Nanjing University of Technology, Nanjing 210009, PR China.*

†Electronic Supplementary Information (ESI) available: [experimental, Ag3d XPS spectra of the AgNCs-AD, and TEM image of the formed different sizes of monodisperse NaCl crystals, Ag@NaCl, AgNCs-AD and AgNPs are available]. See DOI: 10.1039/c000000x/

1 A. R. Tao, Nature Photon., 2014, **8**, 6-8.

2 X. Xia, J. Zeng, B. McDearmon, Y. Zheng, Q. Li and Y. Xia, *Angew. Chem.*, 2011, **123**, 12750-12754.
3 J. M. Slocik, A. O. Govorov and R. R. Naik, *Nano Lett.*, 2011, **11**, 701-705.
4 H.-L. Jiang, T. Akita, T. Ishida, M. Haruta and Q. Xu, *J. Am. Chem. Soc.*, 2011, **133**, 1304-1306.
5 F. Frederix, J.-M. Friedt, K.-H. Choi, W. Laureyn, A. Campitelli, D. Mondelaers, G. Maes and G. Borghs, *Anal. Chem.*, 2003, **75**, 6894-6900.
6 K. Y. Koltunov and V. Sobolev, *Adv. Chem. Lett.*, 2013, **1**, 280-285.
7 M. Ozbek, I. Onal and R. Van Santen, *J. Catal.*, 2011, **284**, 230-235.
8 A. Yin, X. Guo, W. Dai and K. Fan, *Chem. Commun.*, 2010, **46**, 4348-4350.
9 Y. Lu and K. Chou, *Nanotechnology*, 2010, **21**, 215707.
10 Y. Sun and Y. Xia, *Science*, 2002, **298**, 2176-2179.
11 B. J. Wiley, S. H. Im, Z.-Y. Li, J. McLellan, A. Siekkinen and Y. Xia, *J. Phys. Chem. B*, 2006, **110**, 15666-15675.
12 Y. Tang, Z. Jiang, G. Xing, A. Li, P. D. Kanhere, Y. Zhang, T. C. Sum, S. Li, X. Chen and Z. Dong, *Adv. Funct. Mater.*, 2013, **23**, 2932-2940.
13 O. Akhavan, *J. Colloid Interface Sci.,* 2009, **336**, 117-124.
14 A. Gonzalez, J. Reyes-Esqueda and C. Noguez, *J. Phys. Chem. C*, 2008, **112**, 7356-7362.
15 Y.-K. Lai, J.-Y. Huang, H.-F. Zhang, V.-P. Subramaniam, Y.-X. Tang, D.-G. Gong, L. Sundar, L. Sun, Z. Chen and C.-J. Lin, *J. Hazard. Mater.*, 2010, **184**, 855-863.
16 R. C. Tolman, *J. Chem. Phys.*, 1949, **17**, 333-337.
17 X. Jiang and C. J. Brinker, *J. Am. Chem. Soc.*, 2006, **128**, 4512-4513.
18 X. Jiang, T. L. Ward, F. v. Swol and C. J. Brinker, *Ind. Eng. Chem. Res.*, 2010, **49**, 5631-5643.
19 O. Abdulrahman, *Catal. Sci. Technol.*, 2012, **2**, 800-806.
20 Z. Zhang, C. Shao, Y. Sun, J. Mu, M. Zhang, P. Zhang, Z. Guo, P. Liang, C. Wang and Y. Liu, *J. Mater. Chem.*, 2012, **22**, 1387-1395.
21 S. Wunder, F. Polzer, Y. Lu, Y. Mei and M. Ballauff, *J. Phys. Chem. C*, 2010, **114**, 8814-8820.
22 M. A. Mahmoud, R. Narayanan and M. A. El-Sayed, *Acc. Chem. Res.*, 2013, **46**, 1795-1805.